
철근콘크리트 보의 휨전단균열 발생 메카니즘에 대한 연구

Flexural-Shear Cracking Mechanism in Slender Reinforced Concrete Beams



김 우*
Kim Woo

ABSTRACT

This paper describes an experimental investigation into the cause of critical-shear cracking in slender reinforced concrete beams, utilizing sixteen simply supported reinforced concrete beams loaded to failure. The basic approach used was that the test beams were specially designed and fabricated to artificially isolate or add the effect of a certain factor on the critical-shear cracking process. Then these test results were compared with results from ordinary control beams, and the differences were analyzed to deduce the major cause for the initiation and the propagation of flexural-shear cracking. The results indicated that the initiation of flexural-shear cracking was strongly associated with the bond between concrete and reinforcement. Also, it was found that the propagation of the critical shear crack depended exclusively on the intensity of horizontal cracking. Some results were incompatible with the concept of shear strength of critical sections that forms the basis of current shear design provisions. A more rational hypothesis of bond-induced shear failure mechanism is derived based on these experimental results.

Keyword : beam(supports); bond; cracks; failure; reinforced concrete; shear failure.

* 정회원, 전남대학교 토목공학과 부교수

• 본 논문에 대한 토의를 1998년 10월 31일까지 학회로 보내주
시면 1998년 12월호에 토의회답을 게재하겠습니다.

1. Introduction

The shear failure of slender reinforced concrete beams is characterized by the occurrence of a flexural-shear crack (inclined shear crack)^{1,2}. This crack develops after the onset of nearby flexural cracking; thus the initial flexural cracks greatly influence the stress redistribution that follows the development of the flexural cracks. Hence, attempts to quantify analytically the mechanism of flexural-shear cracking have not been successful to date. In addition, since shear failures of beams without web reinforcement are brittle in nature, experimental observations have provided insufficient information on the shear failure process in spite of the large number of previous laboratory investigations. Considerable differences in opinion exist regarding the flexural-shear cracking mechanism in reinforced concrete beams.

The present work explores the fundamental cause of flexural-shear failure in slender reinforced concrete beams. This work is based on a comparative study of strength and deformational characteristics, as well as fracture processes, of various reinforced concrete beams with the same overall geometry and loading conditions, but with selectively different features such as debonding of reinforcement over part of its length, support conditions that do not provide restraint, and shear reinforcement at carefully defined locations. Attention herein was focused mainly on inclined shear cracking: the mechanism of inclined shear crack initiation and the manner of inclined shear crack propagation for beams with shear span-to-depth ratios ranging from 1.5 to 4.0.

2. Experimental Program

2.1 Design of test specimens

The test beams consisted of 16 rectangular concrete beams, each 127 mm wide and 230 mm deep, with two-D16 high strength bars as tension reinforcement (steel ratio = 0.0165).

The effective depth was 190 mm. Symmetrical 2-point loads gave shear span-to-depth ratio a/d values from 1.5 to 4. This experimental investigation included 5 series of specimens as outlined in Table 1, with the first series of 5 beams forming the control specimens. The CNB series (control normal beams) consisted of 5 normal beams to provide a basis of comparison for subsequent test results. The results were designated as the control value for reference purpose. The variable was the shear span ratio, with values of 1.5, 2.0, 2.5, 3.0, and 4.0. Each of the other 4 series had different feature, which was specially designed and fabricated to isolate or add the effect of a certain factor on shear behavior as followings:

- UBB series (beams with unbonded bars) —Four beams were used to investigate the effect of unbonded tension reinforcement. The bond between the steel and the concrete was artificially eliminated over selected lengths of the reinforcement along the shear span using lengths of PVC pipe covers. Three beams had a/d of 3, and the other had a/d of 4. The variable in this series was the length and location of unbonded zone along the tension bar, as shown in Fig. 1(b).

- NRC series (beams with no reaction confinement)—Two beams were designed to explore the effect of support reaction confinement. The support reactions were not directly transferred to the bottom surface of

the beams. As shown in Fig. 1(c), the reactions were resisted by the corbels that projected from the side faces of the beam. The corbel on either side was attached only at upper portion of the side face, and separated at the bottom portion around the steel level up to 64 mm from the beam lower face.

• CHC series (beam with confined horizontal cracking) – Horizontal cracking was confined with prestressed external stirrups (so-called clamps), as shown in Fig. 1(d). The clamps were placed on the section at the one third point of either shear span, which was the most probable section of horizontal crack initiation.

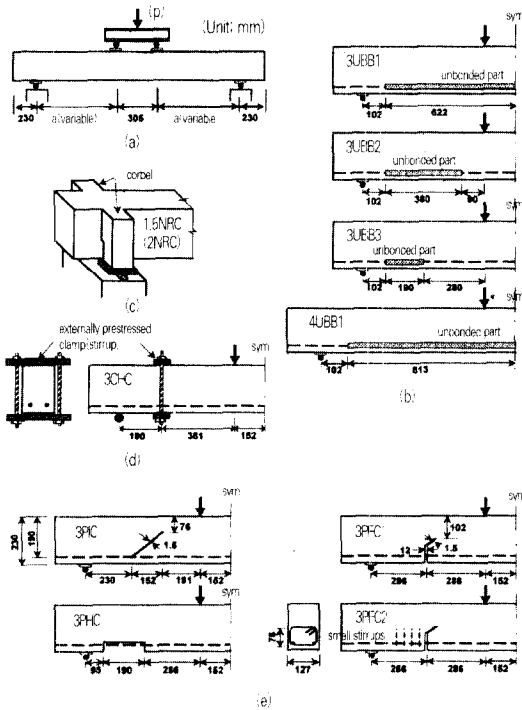


Fig. 1 Geometrical configurations of Test Specimens:
 (a) Schematic layout of test setup,
 (b) Beams in UBB series
 (c) Details of the support in NRC series,
 (d) Beam in CHC series,
 (e) Beams in P series

• P series (beams with preformed crack) – Four beams (each with $a/d = 3$) were made to have artificial preformed crack. As shown in Fig. 1(e), three different types of crack were prefabricated: inclined crack in 3PIC, horizontal crack in 3PHC, and flexural crack in 3PFC1 and 3PFC2.

2.2 Materials, loading, and instrumentation

The concrete mixes used were designed to develop cylinder compressive strength of 31 MPa (320 kg/cm^2) at 28 days. The cement was commercial Portland cement Type I. The sand was a local product from a glacial alluvial deposit: it consisted mainly of quartz and had a fineness modulus of 2.60. The gravel was crushed limestone with a maximum size of 12.5 mm. The materials were batched by weight: the water to cement ratio was 0.58, and the cement to sand to gravel ratio was 1 : 3 : 3. The reinforcing steel was commercially available deformed bars. D16 bars were used for longitudinal reinforcement, with the actual yield strength = 461 MPa (4720 kg/cm^2). After casting, the specimens and test cylinders were covered with plastic sheeting and kept moisture for seven days. Tests were performed 21 to 28 days after casting.

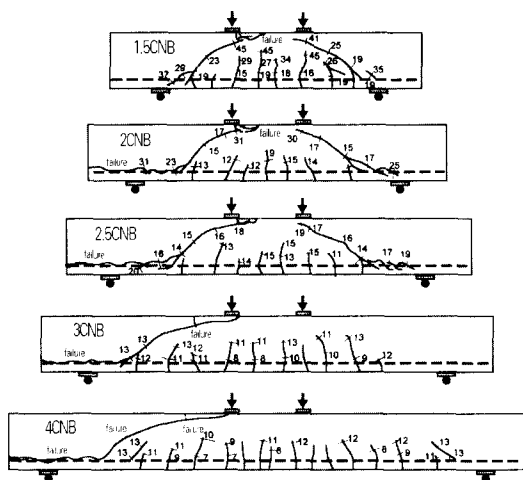
3. Results and Discussion

The main results are summarized in Table 1. The shear cracking load P_{cr} was the applied load at which the inclined shear crack was first observed, and the ultimate load P_u was the maximum load measured during each test. Since the concrete compressive strengths ranged from 26.5 MPa to 37.7 MPa, the test results were modified to allow individual tests to be compared on

an equal basis. Modified ultimate loads P_{mu} were obtained by normalizing the test results with respect to a nominal concrete strength of 31 MPa, using the assumption that, within the concrete strength range used, shear strength was proportional to the square root of the compressive strength. Thus, the shear cracking loads as well as the failure loads were multiplied by $\sqrt{31/f'_c}$

3.1 Effect of a/d Ratio

Fig. 2 shows the crack patterns in the CNB series beams. The critical shear crack



The numbers denote extent of cracking at the given loads in kips. 1 kip = 4.45kN

Fig. 2. Crack configurations of beams in CNB series

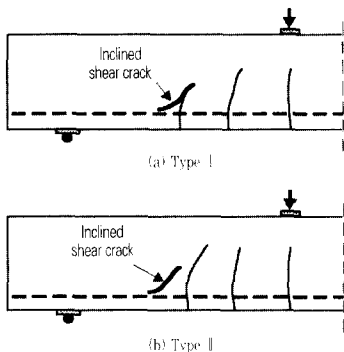


Fig. 3. Pattern of inclined shear crack initiation observed

initiation process was the same in all beams regardless of a/d ratio. After the formation of the flexural cracks, a distinct diagonal crack appeared suddenly a short distance above the tension steel and in the vicinity of the outermost previously developed flexural crack, as shown in Fig. 3.

This initiation of shear cracking observed in the tests was quite different from the inclined extension of an ordinary flexural crack. Then as the load increased, this crack propagated further in both directions. At the upper end it extended toward the load point, and at the t propagated downward across the steel or along the steel. For the convenience of the present study, the upward branch of this critical crack was called an inclined shear crack, and the downward branch was called a horizontal crack.

In all beams in CNB series, the crack propagation rate into the compression zone with increase of load, however, differed greatly with the a/d variation. Correspondingly, the ultimate failure in the compression zone took different forms. In the shorter beams 1.5CNB and 2CNB, the horizontal crack did not form distinctly and the upward inclined shear crack was stable, resulting finally in crushing failure at the compression zone (shear-compression failure). In the longer beams 3CNB and 4CNB, the inclined shear crack propagated in an unstable manner as soon as it initiated, resulting in sudden failure by separation of the beam into two parts (diagonal-tension failure). Thereby, the reserve strength P_r (defined herein by difference in load between P_{cr} and P_u) varied considerably with the variation of a/d ratio as illustrated in Fig. 4, and tabulated in Table 1.

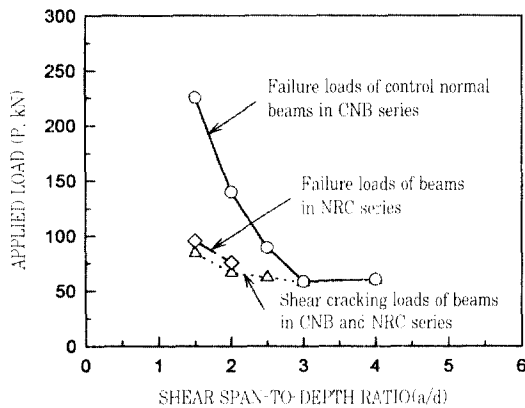


Fig. 4 Variation of cracking and failure loads of beams in CNB and NRC series

Table 1 Test results

Series	Specimen	Concrete strength f_c MPa	Shear span ratio a/d	Measured values			Modified ultimate load ¹⁾ P_u^* kN	Relative strength	
				Shear cracking load P_c kN	Ultimate load P_u kN	Reserve strength ²⁾ P_r kN		Shear strength ratio P_c/P_u	Flexural strength ratio M_u/M_c
CNB	15CNB	30.1	1.5	84.5	225.5	140.0	228.8		1.08
	20CNB	30.1	2.0	66.7	140.1	73.4	122		0.89
	25CNB	30.1	2.5	62.3	89.4	27.1	90.7		0.71
	30CNB	37.7	3.0	37.8	58.7	0.9	53.2		0.54
	40CNB	34.9	4.0	60.5	60.5	0.0	60.0		0.75
UBB	3UBB1	27.1	2.0	-	96.5	-	63.2	1.94	0.94
	3UBB2	33.6	3.0	-	110.3	-	65.9	1.99	1.04
	3UBB3	30.1	3.0	-	64.9	-	65.8	1.24	0.62
	4UBB1	28.4	4.0	-	76.1	-	79.6	1.32	0.98
NRC	15NRC	28.4	1.5	85.0	95.6	10.6	89.7	0.44	0.46
	20NRC	30.1	2.0	66.0	76.1	10.1	77.2	0.54	0.49
CHC	3PFC	35.8	3.0	60.0	60.0	0.0	60.4	1.01	1.01
P	3PFC	36.6	3.0	-	72.1	-	31.6	0.87	0.49
	4PFC	29.4	3.0	-	58.5	-	49.3	0.74	0.57
	3PFC1	31.6	3.0	-	52.5	-	51.9	0.98	0.50
	3PFC2	34.9	3.0	-	74.7	-	70.6	1.33	0.56

* Difference in load between the shear cracking load and the ultimate load.

¹⁾ Modified strengths obtained by normalizing the test data with respect to a nominal concrete strength of 31 MPa.

²⁾ P_r (net shear strength) (This is the modified ultimate failure load of each control normal beam as the basis of comparison).

- - The measured maximum moment at beam failure ($M_u = aP_u/20$).

+ + + The nominal flexural strength for the specimen calculated by ACI rectangular stress block approach.

3.2 Effect of unbonded reinforcement

The primary objective of the beams with unbonded bars (UBB) series was to study the effect of unbonded lengths along the tension reinforcement on shear crack pattern and load carrying capacity. The recorded

crack patterns for these beams are shown in Fig. 5, and the load-deflection curves are compared with that of the control normal beam in Fig. 6.

In beams 3UBB1 and 4UBB1 [whole span except anchorage bond length was unbonded as in Fig. 1(b)], one or two flexural cracks formed in the pure moment zone at very early stage of loading. The cracks opened extremely wide and extended deep into the compression zone with increasing load. Flexural stiffness was less than that of the control normal beam, and crushing occurred progressively in the compression zone, with accompanying large deformation and formation of hinging, as represented by the load-deflection curve for 3UBB1 in Fig. 6. The ultimate loads for 3UBB1 and 4UBB1 were 96.5 kN and 76.1 kN respectively, which were 94 % and 98 % of their nominal flexural strengths as summarized in Table 1.

In beams 3UBB2 and 3UBB3 [bond along a part of the reinforcement in the shear span was artificially eliminated, as in Fig. 1 (b)], the first flexural crack formed at the interior end of the unbonded region in the shear span at a very early loading stage. With further increase of load, the first flexural crack in the shear span extended deep into the shear compression zone, opened widely, and then stabilized. The failure of 3UBB2 occurred by crushing in the compression zone when the load reached 110.3 kN, which was 104 % of its calculated nominal flexural capacity, and nearly twice of the ultimate load of the control normal beam 3CNB. One important fact observed in 3UBB2 was that the first flexural crack in the shear span, although it was inclined as a typical flexural-shear crack and opened extremely widely, did not become the critical crack which

governed the failure of the beam.

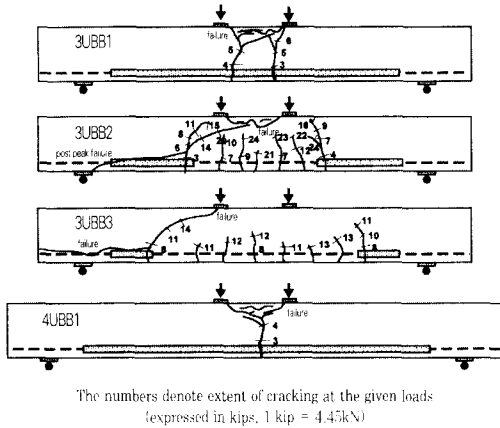


Fig. 5 Crack configurations of beams in UBB series

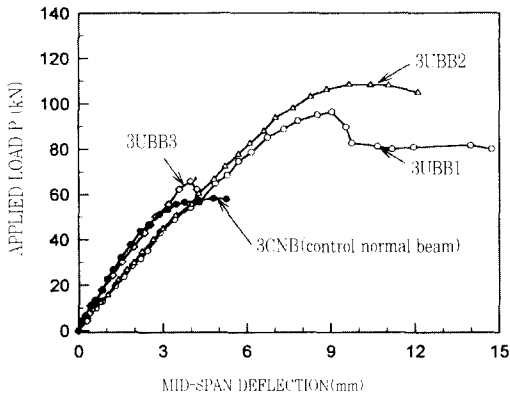


Fig. 6 Comparison of load-deflection curves of beams in UBB series with that of control normal beam (3CNB)

The critical inclined crack in 3UBB3 formed at lower load stage, developed much more extensively, and opened far more widely because the bars were unbonded. Consequently, the aggregate interlocking became less effective; thus, in turn, increasing the shear carried by the remaining uncracked concrete above the crack tip as well as the dowel shear. Hence, smaller shear carrying capacity should have been expected. Nevertheless, the actual failure load was 24% higher than that in the

control normal beam 3CNB.

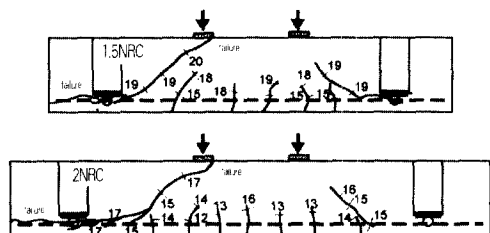
From the above test results, it is evident that the critical inclined crack in 3UBB2 and 3UBB3 was fundamentally different from that in 3CNB although the cracks were nearly identical in overall geometry. The former was stable, and the latter was unstable. Thus the elimination of bond resulted in a drastic change in failure mode as well as a large increase in load capacity. This experimental evidence indicates that the bond between concrete and reinforcement is a critical factor in flexural-shear cracking in reinforced concrete beams.

3.3 Effect of released horizontal cracking

Since an inclined shear crack produces effects conducive to further localization of internal stresses, any inclined shear crack in a beam is potentially dangerous. However, initiation of an inclined shear crack does not, of itself, mean complete rupture of the beam, as evidenced by high reserve strength in some beams having a short shear span. As illustrated in Fig. 4, the shorter beams 1.5CNB and 2CNB showed a large reserve strength. It is believed that the stability of an inclined shear crack is related to the degree of horizontal cracking along the tension steel. In the short beams, 1.5CNB and 2CNB, horizontal cracking was naturally restricted by the support reaction pressure as soon as it initiated because the section at which the crack started was quite close to the support. This also stabilized the upward inclined crack so that high reserve strength resulted. To study this issue, two beams, 1.5NRC and 2NRC, were designed to artificially eliminate the support bearing confinement effect and thus allow extensive horizontal cracking. As shown in Fig. 1(c),

the beams were supported on their sides with no support force acting on the lower face of the beams.

The crack configurations of NRC series are shown in Fig. 7, and the load-deflection curves are compared with those of the corresponding control normal beams in Fig. 8. In the early loading stage up to the shear cracking load, the crack pattern was quite similar to that of its control normal beam. Furthermore, the slopes of the load-deflection curves were identical to those of the control beams up to the shear cracking load as shown in Fig. 8. This indicated that the change of the support system in NRC series did not alter the behavior of a normal beam at early loading stages.



The numbers denote extent of cracking at the given loads (expressed in kips, 1 kip = 4.45kN)

Fig. 7 Crack configurations of beams in NRC series

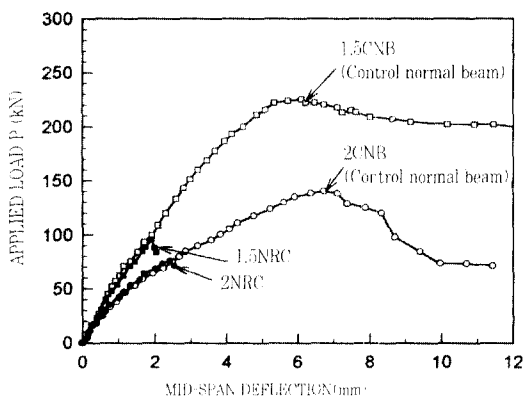


Fig. 8 Comparison of load-deflection curves of beams in NRC series with those of control normal beams

After the inclined shear crack formed,

however, the behavior of the NRC beams was fundamentally different from that of the control beams. In the beams without support reaction confinement, 1.5NRC and 2NRC, the initiated inclined shear crack extended very fast at both ends of the crack, toward the loading point and along the tension steel forming a distinct horizontal crack. Thereby the beams were ruptured by total separation in a brittle diagonal tension failure mode when the load reached 95.6 kN for 1.5NRC and 76.1 kN for 2NRC, giving reserve strengths of about 10 kN. These load-carrying capacities were only 44 % and 54 % of those in their corresponding control normal beams.

The results of these tests show that the elimination of the support reaction confinement in short span beams led to extensive horizontal cracking along the reinforcement, with premature failure at greatly reduced load capacities. Thus the from shear compression type to diagonal tension type, and resulted in negligibly small reserve load carrying capacity.

3.4 Effect of confined horizontal cracking

In the contrast to the shear behavior of the beams with short shear span ($a/d < 2.5$), the longer span beams ($a/d \geq 3$) had inclined cracks that propagated through the entire section with zero or negligibly small reserve load, as illustrated in Fig. 4. The author postulated that the instability of the shear crack in the longer shear span beams was attributed to extensive horizontal cracking at the level of the reinforcement. In order to verify the assumption, the beam 3CHC was designed and built to suppress the horizontal cracking by providing an external prestressed clamp (stirrup) at outer third section of the shear span [see Fig. 1(d)], which was the

most probable location for a horizontal crack initiation (as occurred in 3CNB). Cracking behavior is shown in Fig. 9

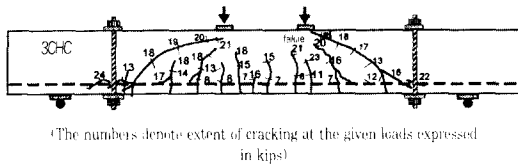


Fig. 9 Crack configuration of beam 3CHC

Comparing the results for this beam 3CHC with that of the control normal beam 3CNB, at loadings below the shear cracking load, the cracking patterns at given load levels were the same. However, the rate of the shear crack propagation into the compression zone differed greatly. In 3CHC the inclined shear crack extended very slowly into the compression zone with increasing load, requiring a large additional load of 49 kN for failure by crushing in the compression zone at 109 kN, almost twice the capacity of 3CNB and equal to the full flexural load-carrying capacity of the section as indicated by the flexural strength ratio of 1.01 in Table 1. Some of this increase of strength might be attributed to the increase of the dowel resistance due to the external stirrups provided.

3.5 Effect of preformed crack

Four beams in the P series were tested to study the effect of various preformed cracks. The resulting crack patterns are shown in Fig. 10, and the measured loads are summarized in Table 1. In 3PIC, an artificial inclined crack was prefabricated at the middle of each shear span to closely simulate the actual inclined crack observed in the control normal beam 3CNB [see Fig. 1(e)]. As loading progressed, a horizontal crack started from the bottom end

of the preformed crack at 31 kN. At 33 kN the upward crack formed at the upper end of the preformed crack, then stabilized with accompanying large deformation. When the load reached 52.1 kN, the beam failed by sudden disintegration of the concrete at the right loading point. This failure load was only 3 % lower than in the control normal beam 3CNB, even though most of the aggregate interlocking resistance was eliminated because of the prefabricated crack. It should be noted that conventional approaches to shear capacity would infer that the aggregate interlocking shear resistance should account for approximately 50 % of the total shear resistance of a beam (according to Ref. 3).

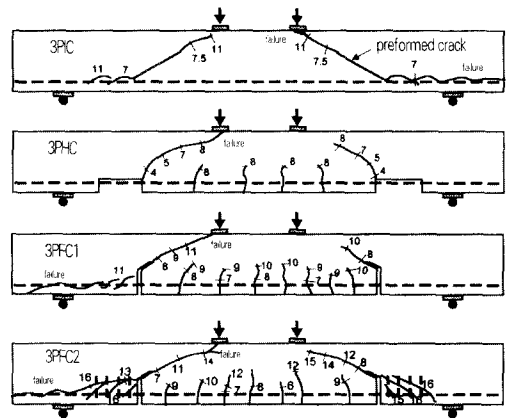


Fig. 10 Crack configurations of beams in P series

In 3PHC, a concrete portion 51 mm depth and 190 mm length at the center of each shear span was blocked out to simulate the effect of a horizontal crack as well as to lessen dowel stiffness. With the application of load, the first crack formed at the inward end of each notch at very low load levels. With increasing load, this crack extended gradually and penetrated the whole depth

when the load reached 38.3 kN, which corresponded to 74 % of the shear strength of the control normal beam 3CNB.

In 3PFC1 and 3PFC2, an artificial flexural crack, which was 127 mm high and slightly bent at the top of the crack to simulate a real flexural crack in the shear span as shown in Fig. 1(e), was formed into both shear spans of each beam. 3PFC2 was designed to restrict horizontal cracking by providing small stirrups in the exterior half of each shear span. In both beams, although the prefabricated flexural crack started to extend at an early loading stage because of the stress raiser effect at the tip, this crack was stable until the horizontal crack started to propagate. As the horizontal crack extended toward the support, the upward extension of the preformed crack approached the loading points. The beam 3PFC1 failed at 98 % of P_u in 3CNB, even though a substantial part of the interlocking shear portion was eliminated by the preformed crack. Moreover, the load carrying capacity of the beam 3PFC2 was 33 % higher than that of the intact beam 3CNB. The primary reason for this strength increase was attributed to the effect of confined horizontal cracking due to the small stirrups provided. From these results, it can be said that an inclined flexural crack, by itself, without any horizontal crack along the reinforcement, cannot become critical, and that horizontal cracking is a prerequisite for beam failure in shear.

4. Bond-Induced Shear Failure Mechanism

The present experimental results provide some clues to help explain the major cause and the process for the initiation and

propagation of shear cracking in reinforced concrete beams.

The bond forces existing between the two different materials (concrete and steel) would appear to be the primary cause for the initiation of the shear crack, and its propagation into the compression zone may well be an after-effect of the horizontal cracking along the longitudinal reinforcement. Incorporating this experimental observation with mechanics principles, a behavioral model is driven for the critical shear cracking, and then the model is applied to more fully explain the behavior obtained from the present experiments.

4.1 Initiation of shear crack

According to the present tests as well as other tests on reinforced concrete beams under point loading, the manner by which the shear crack initiates has certain common characteristics: Shortly after the onset of flexural cracking in the shear span, a small distinct diagonal crack suddenly appears a short distance above the longitudinal reinforcement, and in the vicinity of a previously developed flexural crack, as illustrated in Fig. 3. Therefore, the state of shear stress in a reinforced concrete beam is examined when the beam is loaded to the level that produces some flexural cracking and incipient shear cracking just outside the flexurally cracked region.

A two-point loaded reinforced concrete beam of rectangular cross section after formation of some flexural cracks is shown in Fig. 11(a). Since the beam has both a bending moment M and a shear force V acting on the shear span, the shear stress can be calculated from the equilibrium of an element $opqr$ [Fig. 11(b)] taken from the

lower end segment of the free body diagram. The horizontal shear force acting on the shear surface $q-r$ is vba , where v = average shear stress. From horizontal equilibrium of the forces on the element $opqr$, this shear force equals the reinforcement tension force T at the flexural crack section $p-r$. Hence the average shear stress v on the horizontal plane is: $v = T / (b a)$. The principle behind this equation is identical to that in an elastic homogeneous beam, but the value of shear stress v in the concrete beam needs very careful consideration because of the discontinuities produced by cracking and the complexities in stress distribution produced by composite action of the two materials.

Since the reinforcement force T is transferred to the concrete through bond, and the shear surface $q-r$ is close to the level

of the longitudinal reinforcement, the shear stress distribution on the surface is highly dependent on the bond phenomena. Recognizing that the element $opqr$ in Fig.11(b) is analogous to a simple pullout bond test specimen having special boundary conditions, the approximate state of shear stress due to the bond may be determined.

For the condition that the stress level of the embedded bar is below yield, the pullout bond test results show that maximum bond stress occurs near the loaded end (at surface $p-r$ in Fig. 11(b) in the present case), with ratio of maximum bond stress to average bond stress of much more than 2 according to Ref. 4. Hence the distributions of the shear stresses along the surface $q-r$ and $s-t$ are the forms shown in Fig. 11(c) and (d) respectively. This argument implies that immediately after the flexural crack $p-r$ forms, the bond phenomenon leads to highly concentrated shear stress in the zone above the reinforcement and adjacent to the crack.

The important point to be made above is the substantial magnification of shear stress in the zone slightly above the reinforcement and near the outermost flexural crack (the critical zone in Fig. 11(a)) from the effects of the local bond stress concentration. This zone of the local shear stress concentration coincides well with the experimentally observed zone of shear crack initiation (see Fig. 3). In view of the above, with no bond between the concrete and the reinforcement in the shear span zone of the beams in UBB series, the bond-induced shear stress was absent, and a shear crack did not form, resulting in the avoidance of a shear failure.

In view of the above, it is concluded that the nature of local bond stress concentration immediately after flexural cracking is a

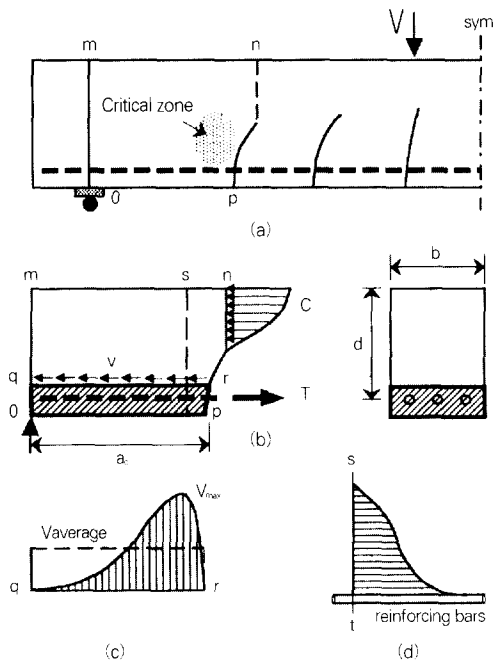


Fig. 11 Shear stress concentration for flexural-shear crack initiation (a) Overall beam configuration prior to shear cracking, (b) Beam end part, (c) Shear (bond) stress distribution along along a horizontal plane $q-r$, and (d) Shear stress distribution along a vertical plane $s-t$

major cause for the initiation of the flexural-shear cracking in reinforced concrete beams. The parallel analytical formulation is described in detail in Ref. 5.

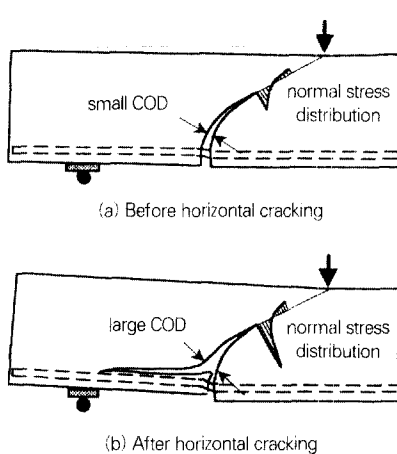


Fig. 12 Effect of horizontal cracking on flexural-shear crack propagation

4.2 Propagation of shear crack

It appears from the present work that the stability of the critical shear crack extending into the compression zone varies with the extent of the horizontal cracking. Hence, a basic concept of fracture mechanics will be applied to explain the effect of horizontal cracking on shear crack extension. In fracture mechanics, crack opening displacement (COD) is an alternative measurement of crack tip stress.⁶ This is because the crack tip strain is related to the COD, which is a measurable quantity. From the above view point, extensive horizontal cracking may result in a large increase of COD at the inclined shear crack mouth zone, while a beam with no horizontal crack has small COD, as conceptually compared in Fig. 12. The increase in the COD at the shear crack mouth zone may result in two major changes in the shear compression

zone ahead the critical shear crack tip: (1) the stress at the crack tip will be higher because the element at the crack tip experiences high strains, and (2) the component of shear force carried by the uncracked concrete will be increased because the widely opened crack width will result in smaller resistance by aggregate interlocking. Based on this observation, an extensive horizontal cracking produces severe modifications of the internal stress system, resulting in sudden increase of the stress at the head of the shear crack. Then, the shear crack becomes unstable, and in turn, is followed by brittle diagonal-tension failure. One of the important characteristics of horizontal cracking along the reinforcement is that, once a horizontal crack starts to extend, the crack extends quickly to the support point without any additional load. This is easily borne out by Fig. 11(b): As the crack extends toward the support, the area of horizontal shearing surface [bac in Fig. 11(b)] resisting load becomes smaller, while the steel tension T stays constant or increases. Thus the horizontal crack is unstable by nature. When this unstable horizontal crack reaches near the support section, it is confined or retarded by the support reaction bearing pressure, as evidenced by the present test results in NRC series.

5. Conclusions

The following conclusions are based on the present experimental investigation into the flexural-shear cracking behavior on slender ordinary reinforced concrete beams without web reinforcement.

1) The initiation of the critical-shear cracking is found to be strongly associated with the magnification of actual shear stress produced by a distinct local stress concentration effect arising

from the formation of the nearby flexural cracks. This local shear stress concentration is produced by the nature of bond between the concrete and the flexural reinforcement.

2) The stability of the critical-shear cracking into the compression zone depends on the extent of the horizontal cracking along the longitudinal reinforcement. Extensive horizontal cracking produces sudden increase of stresses at the head of the inclined shear crack and an unstable propagation mode. The primary factor for the variation of shear strengths and failure modes with respect to a/d is directly related to the intensity of unstable horizontal cracking.

3) The new concept of the bond-induced shear failure mechanism described in this paper may lead to a comprehensive understanding of the causes and mechanisms of flexural-shear cracking failure in reinforced concrete beams in terms of initiation and propagation.

References

1. ASCE-ACI Committee 426. "The Shear Strength of Reinforced Concrete Members." Journal of the Structural Division, ASCE, V. 99, No. ST6, June 1973, pp. 1091-1188.
2. Bresler, B., and MacGregor, J. G.. "Review of Concrete Beams Failing in Shear." Journal of the Structural Division, ASCE, V. 93 No. ST1, Feb. 1967, pp. 343-372.
3. Taylor, H. P. J.. "Investigations of the Forces Carried Across Cracks in Reinforced Concrete Beams in Shear by Interlock of Aggregate." Technical Report 42. 447, Cement and Concrete Association, London, England, 1970, 22 pp.
4. Hungspreug, S., "Local Bond Between a Reinforcing Bar and Concrete under High Intensity Cyclic Load." Structural Engineering Department Report 81-6, Cornell University, Jan. 1981.
5. Kim, W., and White, R. N., "Initiation of Shear Cracking in Reinforced Concrete Beams with No Web Reinforcement." ACI Structural Journal, V. 88, No. 3, May-June 1991, pp. 301-308.
6. Wells, A. A., "Unstable Crack Propagation in Metal, Cleavage and Fast Fracture." The Crack Propagation Symposium, Cranfield, U.K., 1961, pp. 210-230.

요 약

이 논문은 직사각형 단면을 갖는 철근콘크리트 보에서 휨전단균열(Flexural-Shear Crack)의 원인을 규명하기 위해 모두 16개의 보를 실험한 결과를 기술한 것이다.

실험에 이용된 콘크리트보는 전단균열에 영향을 준다고 생각되는 몇가지 요소를 인위적으로 소거 또는 고립되도록 특수하게 제작된 것이다. 이러한 특수보의 실험결과를 같은 재원을 갖는 보통의 정상보의 결과와 직접 비교하여서 그 차이를 분석함으로써 휨전단 균열의 발생원인을 규명하였다. 그 결과, 일반적인

콘크리트보에서의 휨전단균열 발생은 철근과 콘크리트의 경계면의 부착 현상과 매우 밀접한 관련이 있는 것으로 나타났다. 또한, 발생된 휨전단균열의 안정성은 주철근을 따라 발생하는 수평균열의 크기에 직접적인 영향을 받고 있는 것으로 나타났다. 본 연구에서 나타난 몇 가지 사실은 현재 사용중인 전단설계규준의 근본을 이루는 전단 위험단면개념과는 상반되는 것도 있었다. 실험에서 알아낸 사실을 근거로 전단파괴기구에 대한 새로운 가설을 제안하였다. 이 새가설은 지금까지 잘 설명되지 않은 휨전단균열의 발생과 진행에 대한 원인 및 과정을 상당히 잘 설명해주고 있다고 생각된다.

(접수일자 : 1998. 3. 14)